Liver receptor homolog 1 is essential for ovulation

Rajesha Duggavathi,[1,2] David H. Volle,[1] Chikage Mataki,[1] Maria C. Antal,[3] Nadia Messaddeq,[3] Johan Auwerx,[1,3,4,7] Bruce D. Murphy,[2,6] and Kristina Schoonjans[1,4,5]

[1]Institut de Génétique et de Biologie Moléculaire et Cellulaire, CNRS/INSERM/ULP, 67404 Illkirch, France; [2]Centre de Recherche en Reproduction Animale, Faculté de Médecine Vétérinaire, St-Hyacinthe, Québec J2S 7C6, Canada; [3]Institut Clinique de la Souris, 67404 Illkirch, France; [4]Ecole Polytechnique Fédérale de Lausanne, CH-1015 Lausanne, Switzerland

Female fertility requires normal ovarian follicular growth and ovulation. The nuclear receptor liver receptor homolog 1 has been implicated in processes as diverse as bile acid metabolism, steroidogenesis, and cell proliferation. In the ovary, Lrh1 is expressed exclusively in granulosa and luteal cells. Using somatic targeted mutagenesis, we show that mice lacking Lrh1 in granulosa cells are sterile, due to anovulation. The preovulatory stimulus fails to elicit cumulus expansion, luteinization, and follicular rupture in these mice. Multiple defects, including severely reduced transactivation of the Lrh1 target gene, nitric oxide synthase 3, leads to increased intrafollicular estradiol levels in the absence of Lrh1. This further causes dysfunction of prostaglandin and hyaluronic acid cascades and interrupts cumulus expansion. Lack of Lrh1 also interferes with progesterone synthesis because of failure of normal expression of the Lrh1 targets, steroidogenic acute regulatory protein and cytochrome P450 side-chain cleavage. In addition, expression of extracellular matrix proteases essential for ovulation is compromised. These results demonstrate that Lrh1 is a regulator of multiple mechanisms essential for maturation of ovarian follicles and for ovulation. Lrh1 is therefore a key modulator of female fertility and a potential target for contraception.

Supplemental material is available at http://www.genesdev.org.

Received January 21, 2008; revised version accepted May 9, 2008.

Much of mammalian female infertility can be attributed to dysfunction in ovarian folliculogenesis and ovulation. Both processes are tightly controlled by pituitary gonadotropins and locally produced factors, including steroid hormones and growth factors, which act in a coordinated fashion. In the ovary, the two main female hormones that drive these processes—i.e., estradiol-17β and progesterone—have overlapping but clearly distinct functions. Progesterone is required for successful ovulation, as deletion of progesterone receptor (*Pgr*) disrupts ovulation without affecting follicular growth or luteinization (Robker et al. 2000). Estradiol-17β is critical for both follicular growth and ovulation, as mice null for cytochrome P450 aromatase (*Cyp19*) (Fisher et al. 1998) have arrested follicular growth, while enhanced estradiol action has been linked to ovulatory defects (Jablonka-Shariff and Olson 1998; Gershon et al. 2007). Liver receptor homolog 1 (Lrh1, official gene name: Nr5a2), a member of the NR5A subfamily, is highly expressed in the granulosa cells of follicles and in the corpus luteum (CL) (Fayard et al. 2004; Zhao et al. 2007). Although previous in vitro studies were suggestive of a role of Lrh1 in the regulation of steroidogenesis (Mueller et al. 2006; Zhao et al. 2007) and female sex hormone synthesis (Labelle-Dumais et al. 2007; Mendelson and Kamat 2007; Saxena et al. 2007), progress on elucidating the in vivo role in follicular development and ovulation has been hampered by the embryonic lethality of *Lrh1*-null mice (Botrugno et al. 2004; Paré et al. 2004). In the present study, we explored the role of Lrh1 in ovarian follicular development using somatic targeted mutagenesis and show that Lrh1 is a critical regulator of multiple mechanisms essential for maturation of ovarian follicles and for ovulation.

Results and Discussion

Lrh1$^{gc-/-}$ mice are sterile

We generated granulosa-specific mutants (*Lrh1$^{gc-/-}$*) by crossing *Lrh1*-floxed mice (Coste et al. 2007) with mice expressing the Cre-recombinase from the anti-Müllerian hormone receptor-2 locus (*Amhr2$^{Cre/+}$*) (Jamin et al. 2002). Efficient and selective loss of Lrh1 was observed in the granulosa cells of the ovary but not in other organs of Lrh1$^{gc-/-}$ mice, as evidenced by quantitative gene expression analysis in whole ovary and in granulosa cells isolated by laser microdissection (LMD) (Fig. 1A; Supplemental Fig. S1A–C) and immunohistochemistry (Fig. 1B). When subjected to a 6-mo breeding trial, both *Lrh1$^{gc+/+}$* and *Amhr2$^{Cre/+}$* control females proved fertile, with expected frequency of parturition and litter sizes, while no litters were born *to Lrh1$^{gc-/-}$* females (Fig. 1C; Supplemental Fig. S1D). Antral follicles were observed in ovaries of 8- to 10-wk-old mice of both genotypes, but only ovaries from *Lrh1$^{gc+/+}$* mice contained intact and regressed CL, indicative of multiple ovulatory cycles (Fig. 1D). Vaginal cytology showed sequential stages of estrous cycles on consecutive days in *Lrh1$^{gc+/+}$* mice, while *Lrh1$^{gc-/-}$* mice displayed an abnormal pattern suggestive of prolonged estrus and metestrus (Fig. 1E). These results indicated that adult female mice with granulosa cell-specific deletion of *Lrh1* are sterile, due to anovulation.

Follicles of Lrh1$^{gc-/-}$ mice lack preovulatory tissue remodeling

We next used ovarian superstimulation (Fig. 2A) to determine if exogenous gonadotropins could rescue the anovulatory phenotype in the *Lrh1$^{gc-/-}$* mice. As expected,

[*Keywords*: Lrh1; ovulation; granulosa; infertility; estradiol-17β; Nos3]
Corresponding authors.
[5]E-MAIL schoonja@igbmc.u-strasbg.fr; FAX 33-3-88653299.
[6]E-MAIL bruce.d.murphy@umontreal.ca; FAX (450) 778-8103.
[7]E-MAIL auwerx@igbmc.u-strasbg.fr; FAX 33-3-88653233.
Article is online at http://www.genesdev.org/cgi/doi/10.1101/gad.472008.

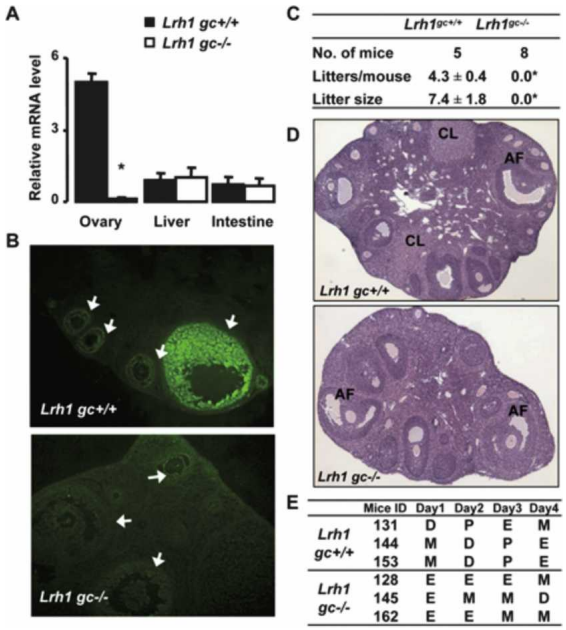

Figure 1. Infertility and anovulation in female granulosa-specific *Lrh1*$^{gc-/-}$ mice. (*A*) Abundance of *Lrh1* mRNA in different tissues of control (*Lrh1*$^{gc+/+}$) and mutant (*Lrh1*$^{gc-/-}$) adult females ($n = 4$ per genotype). (*) $P < 0.001$. (*B*) Demonstration of absence of Lrh1 protein in the granulosa cells of *Lrh1*$^{gc-/-}$ mice. In the *Lrh1*$^{gc+/+}$ mice, Lrh1 expression is exclusive to granulosa cells, and its expression is higher in large follicles relative to small follicles. Arrows indicate follicles of different sizes. (*C*) Reproductive performance of mice of both genotypes in a breeding trial in which females were housed with proven C57BL/6J males for 6 mo. (*) $P < 0.0001$. (*D*) Representative hematoxylin and eosin (HE) staining of ovaries from 8- to 10-wk-old *Lrh1*$^{gc+/+}$ and *Lrh1*$^{gc-/-}$ mice. (AF) Antral follicles; (CL) corpus luteum. (*E*) Representative vaginal smear profiles from *Lrh1*$^{gc+/+}$ and *Lrh1*$^{gc-/-}$ mice. In contrast to control mice, which show normal estrous cycle stages, *Lrh1*$^{gc-/-}$ mice show an abnormal pattern suggestive of prolonged estrus. (D) Diestrus; (P) proestrus; (E) estrus; (M) metestrus.

Lrh1 mRNA levels remained undetectable in *Lrh1*$^{gc-/-}$ granulosa cells from follicles at different stages of gonadotropin-induced growth and differentiation (Fig. 2A; Supplemental Fig. S1E). Interestingly, even upon superstimulation, almost no oocytes could be observed in *Lrh1*$^{gc-/-}$ mouse oviducts 24 h post-hCG administration, while the expected superovulation was induced in *Lrh1*$^{gc+/+}$ mice (Fig. 2B). This supported our hypothesis that the anovulatory phenotype is not due to insufficient gonadotropin concentrations and prompted us to examine follicles 12 h post-hCG, just prior to expected ovulation. At this stage, preovulatory tissue remodeling, dependent on extracellular matrix proteases (Curry and Osteen 2003; Richards et al. 2005), is critical for ovulation and CL formation (Murphy 2000). Histological (Fig. 2C) and electron microscopic (Supplemental Fig. S2A) examinations of ovaries of *Lrh1*$^{gc+/+}$ mice revealed expansion of the theca, the beginnings of focal angiogenic invasion of the granulosa compartment, and changes in the shape of granulosa cells. In contrast, the theca interna in *Lrh1*$^{gc-/-}$ mice remained compact, with no evidence of vascular incursion into the granulosa cells, which were small and round (Fig. 2C; Supplemental Fig. S2B). In addition, analyses of granulosa cells isolated by LMD from antral follicles at defined developmental stages (Fig. 2A) revealed decreased mRNA levels for proteases implicated in the ovulatory process, including a disintegrin-like and metallopeptidase with thrombospondin motif-4 (*Adamts4*), matrix metalloproteinases (*Mmp) 2*, *Mmp9*, and *Mmp19*, but not *Adamts1* in *Lrh1*$^{gc-/-}$ relative to *Lrh1*$^{gc+/+}$ granulosa cells (Supplemental Fig. S2C). Although large antral follicles were present in ovaries of both genotypes (Fig. 2D), expansion of the cumulus oophorus, an event essential for ovulation (Lim et al. 1997; Richards 2005; Gershon et al. 2007), was evident only in *Lrh1*$^{gc+/+}$ follicles and distinctly absent in *Lrh1*$^{gc-/-}$ follicles (Fig. 2D, inset).

Prostaglandin and hyaluronan pathways are disrupted in the absence of Lrh1

LH-induced expression of prostaglandin synthase 2 (*Ptgs2*) and its downstream target, tumor necrosis factor α-induced protein 6 (*Tnfaip6*) in granulosa cells, is required for cumulus expansion (Lim et al. 1997). We found mRNA abundance of *Ptgs2* and *Tnfaip6* to be sub-

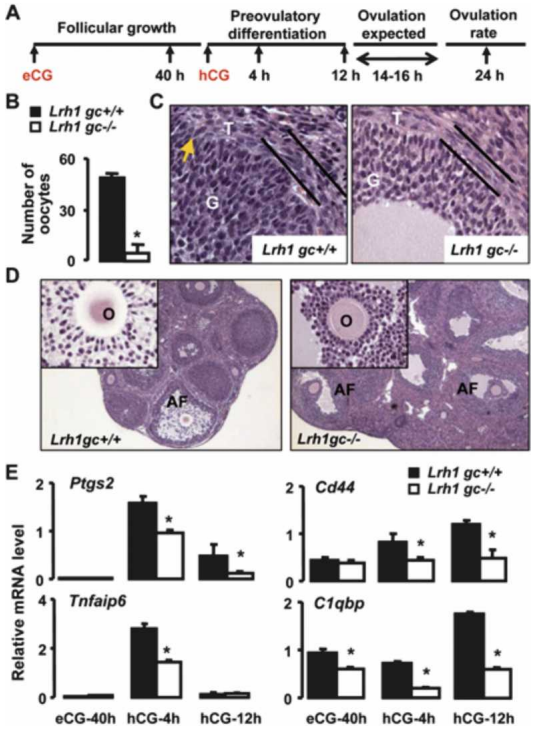

Figure 2. Ovarian superstimulation fails to rescue anovulatory phenotype in *Lrh1*$^{gc-/-}$ mice. (*A*) Immature 3- to 4-wk-old mice were superstimulated with eCG and hCG, and ovaries, granulosa cells, and follicular fluid were collected at specific time points through gonadotropin-stimulated follicular growth and ovulation. (*B*) Ovulation rate in response to superstimulation in immature mice. The number of oocytes in the oviduct was counted in a group of mice at 24 h post-hCG. (*) $P < 0.001$. (*C*) HE staining of *Lrh1*$^{gc+/+}$ and *Lrh1*$^{gc-/-}$ ovaries collected at 12 h post-hCG. Parallel bars demarcate the theca layer; arrow indicates focal invasion of theca into granulosa layer. (G) Granulosa cells; (T) theca cells. (*D*) HE staining of ovaries from superstimulated immature mice collected at 12 h post-hCG. *Inserts* show cumulus granulosa around the oocyte from a preovulatory follicle. (AF) Antral follicles; (O) oocyte. (*E*) Abundance of mRNA for *Lrh1*, *Ptgs2*, *Tnfaip6*, *Cd44*, and *C1qbp* relative to *18S* in *Lrh1*$^{gc+/+}$ ($n = 5$/time point) and *Lrh1*$^{gc-/-}$ ($n = 6$ per time point) granulosa cells. Ovaries were collected at indicated time points during the superovulatory protocol, and the granulosa cells were isolated by LMD. (*) $P < 0.01$.

stantially lower in *Lrh1*$^{gc-/-}$ relative to *Lrh1*$^{gc+/+}$ granulosa cells following hCG stimulation (Fig. 2E), revealing a potential mechanism for failure of cumulus expansion. The hyaluronan (HA) pathway, equally vital for cumulus expansion (Su et al. 2004), also appeared to be compromised. Despite normal expression of hyaluran synthase 2 (*Has2*) (Supplemental Fig. S2D); mRNA abundance of a principal HA-receptor, *Cd44* (Aruffo et al. 1990); and an HA-interacting protein, *C1qbp* (Thakur and Datta 2008) were markedly reduced in *Lrh1*$^{gc-/-}$ relative to *Lrh1*$^{gc+/+}$ granulosa cells (Fig. 2E). Together, these data suggest that dysregulation of prostaglandin and hyaluronan signaling pathways is responsible for defective cumulus expansion in the absence of Lrh1.

Absence of Lrh1 in granulosa cells leads to enhanced bioavailability of estradiol

Recently, enhanced estradiol-17β signaling has been shown to reduce Ptgs2 expression with the consequence of defective cumulus expansion (Gershon et al. 2007). To determine whether changes in estradiol-17β could be an underlying cause of the phenotype observed in *Lrh1*$^{gc-/-}$ ovaries, we examined estradiol-17β levels in follicular fluid samples at defined stages of follicular growth in both genotypes. Follicular fluid from large antral follicles at 40 h post-eCG administration contained 2.5-fold more estradiol-17β in *Lrh1*$^{gc-/-}$ than *Lrh1*$^{gc+/+}$ mice (Fig. 3A). Consistent with these data, gene and protein expression of cytochrome P450 aromatase (*Cyp19*), the enzyme required for estradiol synthesis, was up-regulated in the *Lrh1*$^{gc-/-}$ granulosa compartment at 40 h post-eCG (Fig. 3B,C). The preovulatory stimulus at this stage of follicular growth is known to lead to a sharp decline in follicular fluid estradiol-17β levels (Fitzpatrick et al. 1997). Intriguingly, although both genotypes showed a precipitous decline in estradiol levels in follicular fluid at 12 h post-hCG, estradiol concentrations remained sevenfold higher in *Lrh1*$^{gc-/-}$ mice (Fig. 3A). The LH-driven preovulatory reduction of follicular fluid estradiol-17β concentrations is characterized by a progressive reduction in *Cyp19* expression (Fitzpatrick et al. 1997), but also depends on the prostaglandin-mediated induction of estrogen-specific sulfotransferase, *Sult1e1*, which contributes to reduce estradiol bioavailability (Gershon et al. 2007). In line with the reduced *Ptgs2* expression (Fig. 2E), the induction of *Sult1e1* gene expression was lower in *Lrh1*$^{gc-/-}$ mice compared with *Lrh1*$^{gc+/+}$ mice (Fig. 3D). Thus, in addition to enhanced synthesis, LH-mediated induction of estradiol inactivation is impaired in granulosa cells that lack Lrh1.

In view of the apparent discrepancy between our data showing an inverse correlation between Lrh1 and estradiol-17β, and previous studies reporting *Cyp19* as a target gene of Lrh1 in vitro (for review, see Zhao et al. 2007), we analyzed whether Lrh1 binds the ovary-specific type II promoter of *Cyp19* using ovaries collected at 40 h post-eCG, the time point at which *Lrh1* and *Cyp19* expression is maximum. Surprisingly, after chromatin immunoprecipitation (ChIP) with a specific Lrh1 antibody, no enrichment of the *Cyp19* promoter region encompassing the Lrh1 response element (Lrh1-RE) was observed, indicating that Lrh1 may not be directly required for *Cyp19* expression in granulosa cells of growing follicles (Supplemental Fig. S1F). In addition, the up-regulation of *Cyp19* expression seemed not to be the result of a compensatory

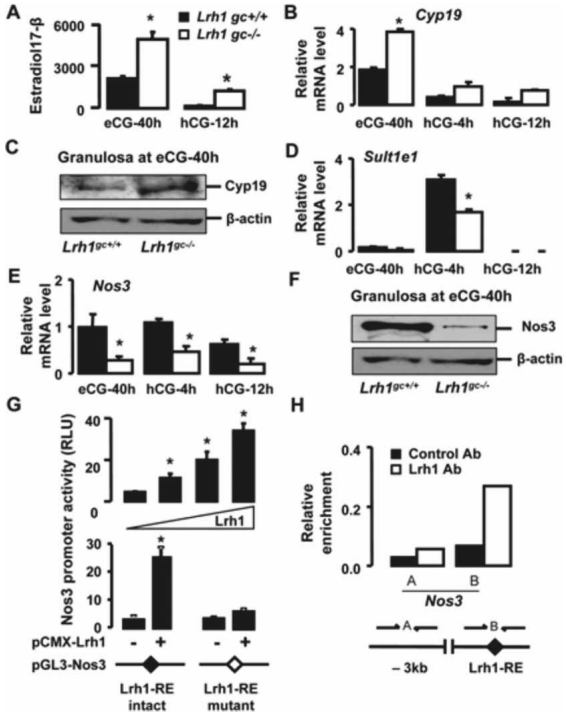

Figure 3. Imbalance in estradiol-17β synthesis and degradation pathways leads to increased estradiol levels in the follicles of *Lrh1*$^{gc-/-}$ mice. (*A*) Estradiol-17β concentrations (nanograms per milliliter) in the follicular fluid of *Lrh1*$^{gc+/+}$ and *Lrh1*$^{gc-/-}$ ovaries ($n = 4$ per genotype). Values were normalized to protein concentration (milligram per milliliter) in the follicular fluid collected. (*) $P < 0.001$. (*B*) Abundance of mRNA for *Cyp19* relative to *18S* in the *Lrh1*$^{gc+/+}$ ($n = 5$ per time point) and *Lrh1*$^{gc-/-}$ ($n = 6$ per time point) granulosa cells. Ovaries were collected at indicated time points during the superovulatory protocol, and the granulosa cells were isolated by LMD. (*) $P < 0.001$. (*C*) Cyp19 immunoblotting performed on *Lrh1*$^{gc+/+}$ and *Lrh1*$^{gc-/-}$ granulosa cell lysates isolated by LMD at 40 h post-eCG. Normalization was done with β-actin. (*D*,*E*) Abundance of mRNA for *Sult1e1* and *Nos3* relative to *18S* in the *Lrh1*$^{gc+/+}$ ($n = 5$ per time point) and *Lrh1*$^{gc-/-}$ ($n = 6$ per time point) granulosa cells. (*) $P < 0.01$. (*F*) Nos3 immunoblot performed on cell lysates from *Lrh1*$^{gc+/+}$ and *Lrh1*$^{gc-/-}$ granulosa cells isolated by LMD at 40 h post-eCG. Normalization was done with β-actin. (*G*) Transient transfection assay of CV-1 cells cotransfected with mouse *Nos3* luciferase reporter and increasing amounts of pCMX-mLrh1 (0–80 ng; *top* panel), and transfection assay of CV-1 cells cotransfected with *Nos3* promoter, containing either intact (GCAAGGGCAT) or mutated (GCAAGTTTAT) Lrh1-RE, together with pCMX-mLrh1(80 ng; *bottom* panel). Normalized luciferase activity was expressed as relative light units (RLU). (*) $P < 0.05$. (*H*) ChIP assay demonstrating the occupancy of Lrh1 on the promoter of *Nos3*. The assay was performed on 40 h post-eCG ovarian extracts using control IgG or Lrh1 antibodies. (Lrh1-RE) The Lrh1 response element is located at –664/–656 upstream of the transcription initiation site.

increase of the closely related receptor steroidogenic factor 1 (Sf1, Nr5a1) (Supplemental Fig. S1G), which has also been shown to regulate *Cyp19* in vitro (for review, see Stocco 2008). Based on these findings, we hypothesized that other mechanisms upstream of estradiol-17β synthesis could be regulated by Lrh1. Interestingly, nitric oxide synthase 3 (*Nos3*) has been reported to negatively affect the expression and activity of Cyp19 in granulosa cells (Snyder et al. 1996; Kagabu et al. 1999). Furthermore, mice null for Nos3 exhibit overproduction of estradiol-17β and defective ovulation (Jablonka-Shariff and Olson 1998), supporting the notion that balanced

estradiol production is required for follicular maturation and ovulation. We found that *Nos3* mRNA levels were considerably reduced in $Lrh1^{gc-/-}$ compared with $Lrh1^{gc+/+}$ granulosa cells during follicular development (Fig. 3E). Likewise, bioactive phosphorylated Nos3 was significantly lower in $Lrh1^{gc-/-}$ granulosa cells at 40 h post-eCG (Fig. 3F), when estradiol production is most pronounced. These data indicate that loss of Lrh1 dramatically reduces Nos3 activity, which, in turn, stimulates Cyp19-mediated estradiol production. To explore whether *Nos3* is a direct target of Lrh1, the ability of Lrh1 to bind and transactivate the promoter of *Nos3* was assessed. In CV-1 cells, ectopic expression of Lrh1 by transient transfection elicited a dose-dependent increase of *Nos3* promoter activity, which was abolished when the putative Lrh1-RE was mutated (Fig. 3G). In addition, ChIP analysis with an Lrh1-antibody revealed strong and specific interaction of Lrh1 with the promoter region encompassing the Lrh1-RE, indicating that Lrh1-mediated induction of the *Nos3* promoter involves direct binding (Fig. 3H). These data identify Nos3 as a novel Lrh1 target upstream of Cyp19-mediated estrogen production and provide, in addition to the observed impact on estradiol metabolism by Sult1e1, a mechanistic basis by which Lrh1 controls estradiol levels.

Lrh1 is essential for transactivation of the genes involved in luteinization

Even though enhanced estradiol action and disrupted prostaglandin signaling lead to defective cumulus expansion and ovulation, they do not appear to disrupt progesterone production and CL formation (Jablonka-Shariff and Olson 1998; Tong et al. 2005). The scavenger receptor B1 (*Scarb1*), steroidogenic acute regulatory protein (*Star*), cytochrome P450 side-chain cleavage (*Cyp11a1*), and 3β-hydroxysteroid dehydrogenase (*Hsd3b*) genes are regulated by Lrh1 in vitro (Schoonjans et al. 2002; Sirianni et al. 2002). All are crucial for progesterone synthesis in granulosa cells in response to LH stimulation (Richards 2005; Miranda-Jimenez and Murphy 2007). The abundance of *Scarb1*, *Star*, and *Cyp11a1*, but not *Hsd3b*, mRNA was consistently lower in granulosa cells of $Lrh1^{gc-/-}$ compared with $Lrh1^{gc+/+}$ mice (Fig. 4A). Owing to the importance of Star in steroidogenesis (Manna et al. 2003; Zhao et al. 2007), we examined its expression as an indicator of luteinization by immunoblotting. Although there was no difference in the level of Star protein in total ovary between $Lrh1^{gc-/-}$ and $Lrh1^{gc+/+}$ mice at 12 h post-hCG, Star protein levels in purified granulosa cells were markedly reduced in $Lrh1^{gc-/-}$ mice (Fig. 4B). The pronounced enrichment of the promoters of *Star* and *Cyp11a1* following ChIP with Lrh1 antibody confirmed that both *Star* and *Cyp11a1* were direct Lrh1 targets (Fig. 4C). Disrupted preovulatory progesterone synthesis in the absence of Lrh1 was further reflected by the lack of an increase in the follicular-fluid progesterone concentration in $Lrh1^{gc-/-}$ mice compared with the remarkable progesterone increase in $Lrh1^{gc+/+}$ mice (Fig. 4D). These data demonstrate that Lrh1 is not only essential for cumulus expansion and ovulation, but is also a key regulator of progesterone production by preovulatory granulosa cells.

In summary, our findings demonstrate that Lrh1 is an essential and pleiotropic regulator of ovarian follicular development and ovulation (Fig. 4E). Since Lrh1, as a nuclear receptor, is a potential pharmaceutical target, the possibility of using Lrh1 inhibitors as contraceptives is attractive given that inhibition of Lrh1 abolishes both ovulation and luteinization, providing a dual mechanism for abrogation of fertility.

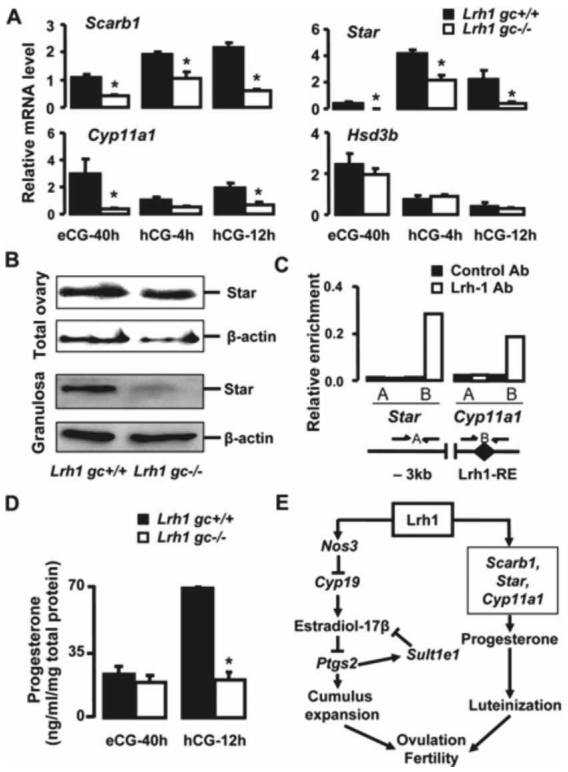

Figure 4. Progesterone production is compromised in $Lrh1^{gc-/-}$ mice. (*A*) Abundance of mRNA for *Scarb1*, *Star*, *Cyp11a1*, and *Hsd3b* relative to *18S* in the $Lrh1^{gc+/+}$ and $Lrh1^{gc-/-}$ ovaries ($n = 4$/genotype/time point). (*) $P < 0.001$. (*B*) Immunoblot for Star in the total extracts from whole ovaries and LMD-purified granulosa cells of $Lrh1^{gc+/+}$ and $Lrh1^{gc-/-}$ mice. Normalization was achieved with β-actin. (*C*) ChIP assay demonstrating occupancy of Lrh1 on the promoters of *Star* and *Cyp11a1*. The assay was performed on 12-h post-hCG ovarian extracts using control IgG or Lrh1 antibodies. (Lrh1-RE) Lrh1 response element at –135/–127 (*Star*) and –50/–41 (*Cyp11a1*) upstream of the transcription initiation site. (*D*) Progesterone concentrations (nanograms per milliliter) in the follicular fluid of $Lrh1^{gc+/+}$ and $Lrh1^{gc-/-}$ ovaries ($n = 4$ per genotype). Values were normalized to protein concentration (milligrams per milliliter) in the follicular fluid collected. (*) $P < 0.001$. (*E*) Scheme representing targets and pathways affected by Lrh1 disruption in granulosa cells. Absence of Lrh1 in the granulosa cells leads to enhanced local estradiol synthesis via down-regulation of its target Nos3, which appears to set in a loop of increased estradiol activity via Ptgs2 and Sult1e1, thereby blocking cumulus expansion. In addition, absence of Lrh1 compromises luteinization process via down-regulation of its steroidogenic targets, including Scarb1, Star, and Cyp11a1. The concomitant defects in cumulus expansion and luteinization lead to anovulation and infertility.

Materials and methods

Animals

Lrh1 floxed ($Lrh1^{L2/L2}$) mice have been described previously (Coste et al. 2007). To generate granulosa-specific Lrh1 mutant ($Lrh1^{gc-/-}$) mice, animals expressing Cre-recombinase from the anti-Müllerian hormone receptor-2 locus ($Amhr^{2Cre/+}$; generous gift of Dr. Richard Behringer) (Jamin et al. 2002) were crossed with $Lrh1^{L2/L2}$ mice. All animal experiments

were approved by the Regional Ethics Committee and performed according to the European Union guidelines.

Estrous cycle detection, breeding trials, and superstimulation protocol
For estrous cycle staging, vaginal lavage in phosphate-buffered saline was collected daily (between 7 and 8 a.m.) on glass slides for each mouse. The slides were stained with May-Grünwald and Geimsa stains to determine estrous cycle stages. For the breeding trial, 8-wk-old *Lrh1*$^{gc+/+}$ and *Lrh1*$^{gc-/-}$ females were housed with reproductively proven C57BL/6J males for 6 mo (two females per male). Cages were inspected daily, and the number and size of litter from each female were noted. For superstimulation, immature (3- to 4-wk-old) mice were administered equine chorionic gonadotropin (5 IU i.p.) followed by human chorionic gonadotropin (5 IU i.p.) 48 h later.

Laser microdissection (LMD)
Serial cryosections (25 µm) of fresh-frozen ovaries were cut at −16°C, thaw-mounted onto PEN slides (Leica), stained with toluidine blue, and dehydrated in 70% and 100% ethanol followed by incubation for 1 h at 37°C. The granulosa cells were excised by LMD (Leica AS LMD) at 20× magnification directly into either RNA-lysis (RNeasy MicroKit; Qiagen) or Laemmli buffer with β-mercaptoethanol. All apparently nonatretic antral follicles in a total of ~50 sections from one ovary were cut for each mouse.

Real-time RT–PCR
Total RNA from tissues and laser microdissected samples was extracted with RNeasy Kits (Qiagen), and reverse-transcribed into cDNA with the SuperScript II First-Strand Synthesis System (Life Technologies) and random hexamer primers. Real-time RT–PCR was performed using SYBR green dye to measure duplex DNA formation with the Roche LightCycler system. Results were normalized to *18S* levels. The sequences of the primer sets used are listed in Supplemental Table 1.

Light and electron microscopy
For histological examination, ovaries were formalin-fixed and paraffin-embedded, cut at 5 µM, and stained with hematoxylin and eosin (HE). Immunohistochemistry was performed on 16 µM cryosections of the ovaries. For transmission electron microscopy, ovaries were processed according to standard procedures (see the Supplemental Material).

Immunoblotting
Total protein extracts from ovaries or laser microdissected granulosa cells obtained with lysis buffer (50 mM Tris-HCl at 7.5, 150 mM NaCl, 1% NP-40, 25 mM NaF with protease inhibitors), were resolved by SDS-PAGE and transferred to nitrocellulose membranes. The blots were probed with the primary antibodies against Lrh1 (Coste et al. 2007), Star (kind donation of Dr. Douglas Stocco), Phospho-Nos3 (Cell Signaling), β-actin (Santa Cruz Biotechnologies), and Cyp19 (Abcam), followed by secondary antibodies against rabbit or goat IgG, and visualized by the Pierce chemiluminescence detection system.

ChIP
ChIP on ovaries using the previously described Lrh1 antibody (Coste et al. 2007) was performed as described in the Supplemental Methods. Amplification of ~100 bp of the distal (control amplicon) or proximal (amplicon encompassing the putative Lrh1 RE) promoter of *Star*, *Cyp11a1*, and *Nos3* was performed using the primer sets listed in Supplemental Table 1. Enrichment of the amplicon normalized to 30-fold-diluted input from immunoprecipitation with Lrh1 antibody and normal rabbit IgG was compared quantitatively.

Transient transfections
The mouse *Nos3* luciferase reporters, containing DNA sequences between −891 and +30 nt from the transcription initiation site, with either an intact or mutated Lrh1 response element (−664/−656), were cloned into the basic pGL3-vector using specific primers (primers for cloning: Forward, 5′-ATCGGAACGCGTGGGCCACTGTGGTGAAGTAT-3′; Reverse, 5′-TACGGAAGATCTGTAGGTGATGCTGCCCACTT-3′ (restriction sites underlined); primers for mutagenesis: Forward, 5′-CCATCTCAGGTGAGGCAAG**TTT**ATTCCGAGGTGAGCACCCA-3′; Reverse, 5′-TGGGTGCTCACCTCGGAAT**AAA**CTTGCCTCACCTGA ATGG-3′). CV-1 cells were transfected with jetPEI (PolyPlus) in 48-well plates. Along with a control β-galactosidase vector (10 ng), luciferase reporter constructs containing either intact or mutated *Nos3* promoters (100 ng) were added in combination with empty pCMX or pCMX-mLrh1 expression vectors (0–80 ng per well). The quantity of DNA was maintained constant by the addition of empty pCMX vector. Cells were harvested 48 h later and assayed for luciferase and β-galactosidase activity. Luciferase values were normalized to β-galactosidase activity.

Radioimmunoassay
Radioimmunoassay for estradiol-17β and progesterone in follicular fluid from ovaries of immature mice collected at 40 h post-eCG and 12 h post-hCG was performed according to the instructions of the manufacturer (MP Biomedicals).

Statistical analyses
Differences between *Lrh1*$^{gc+/+}$ and *Lrh1*$^{gc-/-}$ mice for single point data were determined by Student's *t*-test. For data obtained at multiple time points, two-way analysis of variance was performed. When significant effects of time or genotype or their interactions were obtained, multiple comparisons were made with Tukey's test. All numerical data are represented as mean ± SE. Significant difference was set at $P < 0.05$.

Acknowledgments

We thank Riaz Farooki, Derek Boerboom, and John Eppig for helpful comments on the manuscript; Douglas Stocco for the Star antibody; Richard Behringer for *Amhr2-Cre* mice; and Dorothée Daniel and Tania Meyer for technical assistance. This work was supported by CNRS, INSERM, ULP, Hôpital Universitaire de Strasbourg, ACI, ARC, AFM and PNRHGE (to K.S. and J.A.), and CIHR Grant FRN11018 (to B.D.M.). R.D. was supported by Serono Foundation, Geneva and the Natural Sciences and Engineering Council, Canada.

References

Aruffo, A., Stamenkovic, I., Melnick, M., Underhill, C.B., and Seed, B. 1990. CD44 is the principal cell surface receptor for hyaluronate. *Cell* **61:** 1303–1313.

Botrugno, O.A., Fayard, E., Annicotte, J.S., Haby, C., Brennan, T., Wendling, O., Tanaka, T., Kodama, T., Thomas, W., Auwerx, J., et al. 2004. Synergy between LRH-1 and β-catenin induces G1 cyclin-mediated cell proliferation. *Mol. Cell* **15:** 499–509.

Coste, A., Dubuquoy, L., Barnouin, R., Annicotte, J.S., Magnier, B., Notti, M., Corazza, N., Antal, M.C., Metzger, D., Desreumaux, P., et al. 2007. LRH-1-mediated glucocorticoid synthesis in enterocytes protects against inflammatory bowel disease. *Proc. Natl. Acad. Sci.* **104:** 13098–13103.

Curry Jr., T.E. and Osteen, K.G. 2003. The matrix metalloproteinase system: Changes, regulation, and impact throughout the ovarian and uterine reproductive cycle. *Endocr. Rev.* **24:** 428–465.

Fayard, E., Auwerx, J., and Schoonjans, K. 2004. LRH-1: An orphan nuclear receptor involved in development, metabolism and steroidogenesis. *Trends Cell Biol.* **14:** 250–260.

Fisher, C.R., Graves, K.H., Parlow, A.F., and Simpson, E.R. 1998. Characterization of mice deficient in aromatase (ArKO) because of targeted disruption of the cyp19 gene. *Proc. Natl. Acad. Sci.* **95:** 6965–6970.

Fitzpatrick, S.L., Carlone, D.L., Robker, R.L., and Richards, J.S. 1997. Expression of aromatase in the ovary: Down-regulation of mRNA by the ovulatory luteinizing hormone surge. *Steroids* **62:** 197–206.

Gershon, E., Hourvitz, A., Reikhav, S., Maman, E., and Dekel, N. 2007. Low expression of COX-2, reduced cumulus expansion, and impaired ovulation in SULT1E1-deficient mice. *FASEB J.* **21:** 1893–1901.

Jablonka-Shariff, A. and Olson, L.M. 1998. The role of nitric oxide in oocyte meiotic maturation and ovulation: Meiotic abnormalities of endothelial nitric oxide synthase knock-out mouse oocytes. *Endocrinology* **139:** 2944–2954.

Jamin, S.P., Arango, N.A., Mishina, Y., Hanks, M.C., and Behringer, R.R. 2002. Requirement of Bmpr1a for Mullerian duct regression during male sexual development. *Nat. Genet.* **32:** 408–410.

Kagabu, S., Kodama, H., Fukuda, J., Karube, A., Murata, M., and Tanaka,

T. 1999. Inhibitory effects of nitric oxide on the expression and activity of aromatase in human granulosa cells. *Mol. Hum. Reprod.* **5:** 396–401.

Labelle-Dumais, C., Pare, J.F., Belanger, L., Farookhi, R., and Dufort, D. 2007. Impaired progesterone production in Nr5a2$^{+/-}$ mice leads to a reduction in female reproductive function. *Biol. Reprod.* **77:** 217–225.

Lim, H., Paria, B.C., Das, S.K., Dinchuk, J.E., Langenbach, R., Trzaskos, J.M., and Dey, S.K. 1997. Multiple female reproductive failures in cyclooxygenase 2-deficient mice. *Cell* **91:** 197–208.

Manna, P.R., Wang, X.J., and Stocco, D.M. 2003. Involvement of multiple transcription factors in the regulation of steroidogenic acute regulatory protein gene expression. *Steroids* **68:** 1125–1134.

Mendelson, C.R. and Kamat, A. 2007. Mechanisms in the regulation of aromatase in developing ovary and placenta. *J. Steroid Biochem. Mol. Biol.* **106:** 62–70.

Miranda-Jimenez, L. and Murphy, B.D. 2007. Lipoprotein receptor expression during luteinization of the ovarian follicle. *Am. J. Physiol. Endocrinol. Metab.* **293:** E1053–E1061. doi: 10.1152/ajpendo.00554.2006.

Mueller, M., Cima, I., Noti, M., Fuhrer, A., Jakob, S., Dubuquoy, L., Schoonjans, K., and Brunner, T. 2006. The nuclear receptor LRH-1 critically regulates extra-adrenal glucocorticoid synthesis in the intestine. *J. Exp. Med.* **203:** 2057–2062.

Murphy, B.D. 2000. Models of luteinization. *Biol. Reprod.* **63:** 2–11.

Paré, J.F., Malenfant, D., Courtemanche, C., Jacob-Wagner, M., Roy, S., Allard, D., and Bélanger, L. 2004. The fetoprotein transcription factor (FTF) gene is essential to embryogenesis and cholesterol homeostasis and is regulated by a DR4 element. *J. Biol. Chem.* **279:** 21206–21216.

Richards, J.S. 2005. Ovulation: New factors that prepare the oocyte for fertilization. *Mol. Cell. Endocrinol.* **234:** 75–79.

Richards, J.S., Hernandez-Gonzalez, I., Gonzalez-Robayna, I., Teuling, E., Lo, Y., Boerboom, D., Falender, A.E., Doyle, K.H., LeBaron, R.G., Thompson, V., et al. 2005. Regulated expression of ADAMTS family members in follicles and cumulus oocyte complexes: Evidence for specific and redundant patterns during ovulation. *Biol. Reprod.* **72:** 1241–1255.

Robker, R.L., Russell, D.L., Espey, L.L., Lydon, J.P., O'Malley, B.W., and Richards, J.S. 2000. Progesterone-regulated genes in the ovulation process: ADAMTS-1 and cathepsin L proteases. *Proc. Natl. Acad. Sci.* **97:** 4689–4694.

Saxena, D., Escamilla-Hernandez, R., Little-Ihrig, L., and Zeleznik, A.J. 2007. Liver receptor homolog-1 and steroidogenic factor-1 have similar actions on rat granulosa cell steroidogenesis. *Endocrinology* **148:** 726–734.

Schoonjans, K., Annicotte, J.S., Huby, T., Botrugno, O.A., Fayard, E., Ueda, Y., Chapman, J., and Auwerx, J. 2002. Liver receptor homolog 1 controls the expression of the scavenger receptor class B type I. *EMBO Rep.* **3:** 1181–1187.

Sirianni, R., Seely, J.B., Attia, G., Stocco, D.M., Carr, B.R., Pezzi, V., and Rainey, W.E. 2002. Liver receptor homologue-1 is expressed in human steroidogenic tissues and activates transcription of genes encoding steroidogenic enzymes. *J. Endocrinol.* **174:** R13–R17.doi: 10.1677/joe.0.174R013.

Snyder, G.D., Holmes, R.W., Bates, J.N., and Van Voorhis, B.J. 1996. Nitric oxide inhibits aromatase activity: Mechanisms of action. *J. Steroid Biochem. Mol. Biol.* **58:** 63–69.

Stocco, C. 2008. Aromatase expression in the ovary: Hormonal and molecular regulation. *Steroids* **73:** 473–487.

Su, Y.Q., Wu, X., O'Brien, M.J., Pendola, F.L., Denegre, J.N., Matzuk, M.M., and Eppig, J.J. 2004. Synergistic roles of BMP15 and GDF9 in the development and function of the oocyte-cumulus cell complex in mice: genetic evidence for an oocyte-granulosa cell regulatory loop. *Dev. Biol.* **276:** 64–73.

Thakur, S.C. and Datta, K. 2008. Higher expression of hyaluronan binding protein 1 (HABP1/p32/gC1qR/SF2) during follicular development and cumulus oocyte complex maturation in rat. *Mol. Reprod. Dev.* **75:** 429–438.

Tong, M.H., Jiang, H., Liu, P., Lawson, J.A., Brass, L.F., and Song, W.C. 2005. Spontaneous fetal loss caused by placental thrombosis in estrogen sulfotransferase-deficient mice. *Nat. Med.* **11:** 153–159.

Zhao, H., Li, Z., Cooney, A.J., and Lan, Z.J. 2007. Orphan nuclear receptor function in the ovary. *Front. Biosci.* **12:** 3398–3405.